Magnetic properties of mixed-valence iron phosphate glasses

Hirofumi Akamatsu, Satoshi Oku, Koji Fujita, Shunsuke Murai, and Katsuhisa Tanaka*
Department of Material Chemistry, Graduate School of Engineering, Kyoto University, Nishikyo-ku, Kyoto 615-8510, Japan
(Received 10 June 2009; revised manuscript received 24 August 2009; published 8 October 2009)

Magnetic properties of mixed-valence iron phosphate glasses, where there coexist Fe^{2+} and Fe^{3+} ions, have been investigated. The molar fraction of Fe^{3+} with respect to the total iron ion, $[Fe^{3+}]/[Fe_{total}]$, can be controlled by melting the glass at varied temperatures. Experiments of magnetic aging and memory effects as well as dynamic and static scaling analyses of relaxation time and nonlinear magnetic susceptibility have been performed to get insight into the nature of low-temperature magnetic phase of the glass system. The experimental results reveal that the iron phosphate glasses undergo paramagnet-spin-glass transitions at low temperatures. Temperature dependence of magnetic specific heat suggests that as the temperature is lowered, the magnetic moments start to be frozen at a temperature significantly higher than the spin-glass transition temperature accompanied by a deviation in magnetic susceptibility from Curie-Weiss law. The ratio of the absolute value of Weiss temperature to spin-glass transition temperature increases as the ratio $[Fe^{3+}]/[Fe_{total}]$ becomes larger. This behavior is explainable in terms of the difference in single-ion anisotropy between Fe^{3+} and Fe^{2+} ions.

DOI: 10.1103/PhysRevB.80.134408 PACS number(s): 75.50.Lk

I. INTRODUCTION

A considerable attention has been paid to spin glass because of the expectation that it can be a physical model of random frustrated systems. The extensive search for new spin-glass materials and investigation of their magnetic properties have been performed since Cannella and Mydosh[1] observed magnetic transitions in temperature dependence of susceptibility for binary *Au*Fe alloys with very low concentrations of Fe. A great number of magnetic materials exhibiting the spin-glass behavior have emerged in crystalline alloys, oxides, sulfides, and so forth. Development of experimental, theoretical, and numerical studies on spin glasses has given an insight into their intrinsic nature. Even in this decade, fascinating phenomena involving magnetic aging effects have been reported as unique features of spin glasses.[2–6] Spin glass is also a matter of absorbing interest from the point of view of its analogy to many complex systems such as associative memory in the brain.[7]

Magnetic oxide glass is a prototype of a solid in which magnetic moments are spatially distributed in a disordered fashion like spin glass. In most insulating oxide glasses, magnetic properties are dominated by antiferromagnetic superexchange interaction via an oxide ion. It may be naturally anticipated that all the pairs of magnetic moments antiferromagnetically coupled with each other cannot take their own most stable states because of the random distribution of magnetic ions. In other words, the magnetic frustration is inevitably present in the random structure of oxide glasses. Hence, magnetic oxide glass presumably satisfies the conditions necessary for the spin-glass transition: randomness and frustration.[8] To clarify the mechanism of magnetic transition in oxide glasses, many studies have been performed on temperature dependence of dc and ac magnetic susceptibilities, Mössbauer spectrum, electron-spin-resonance spectrum, and so forth.[9–23] As a result, magnetic oxide glasses, in particular, those containing 3*d* transition-metal ions, have been regarded as a prototype of insulating spin glass. Recently, we have reported that Fe_2O_3-TeO_2 glasses manifest curious phenomena relevant to spin dynamics, including magnetic aging and memory effects as well as critical slowing down similar to those observed in canonical spin glasses.[9] The result strongly confirms that Fe_2O_3-TeO_2 glass system is a typical example of spin glass.

However, there have been few reports about the effect of sorts and chemical states of magnetic ions on the magnetic properties of amorphous insulating spin glasses.[10] One transition-metal ion can take different valence states, leading to the difference in magnetic moment and single-ion anisotropy. For instance, high-spin Fe^{3+} has a $3d^5$ electronic configuration with $S=5/2$ and completely quenched orbital moment, while high-spin Fe^{2+} has a $3d^6$ electronic configuration with $S=2$ and possibly unquenched orbital moment. So, a drastic change in magnetic properties is expected when the valence state of magnetic ion is altered in oxide glasses. This paper focuses on iron phosphate glasses in which the valence state of Fe ion can be either divalent or trivalent. Wedgwood *et al.*[11] performed neutron magnetic scattering for $0.79Fe_2O_3 \cdot P_2O_5$ glass and confirmed that the short-range antiferromagnetic ordering takes place at temperatures as low as 4.2 K. Shaw *et al.*[12] observed spin-glass-like behavior in temperature dependence of dc magnetic susceptibility for $xFe_2O_3 \cdot (100\text{-}x)P_2O_5$ glasses ($30 \leq x \leq 44$, in mol %). Recently we have reported that $57.1FeO \cdot 42.9P_2O_5$ glass exhibits its spin-glass transition at 3.1 K as indicated by its temperature dependent magnetic susceptibility.[13] However, detailed magnetic properties of iron phosphate glasses have not been investigated; especially, the dependence of magnetic behavior on the valence state of iron ions has not been discussed at all.

In this paper, the iron phosphate glasses with varied $[Fe^{3+}]/[Fe_{total}]$ molar ratio have been prepared by melting in an alumina or a glassy carbon crucible at various temperatures, and their magnetic properties have been investigated in detail. These experimental procedures are described in Sec. II. In Sec. III, the valence state of Fe ion and the local structure of Fe ion are discussed in terms of ^{57}Fe Mössbauer

spectroscopy. In Sec. IV, we present the results of magnetic-susceptibility measurements and analyze the data on the basis of Curie-Weiss law and scaling law. Here, the spin-glass behavior of iron phosphate glasses is indicated by not only the magnetic aging and memory experiments but also the dynamic and static scaling analyses of relaxation time and nonlinear magnetic susceptibility. In Sec. V, we describe the results of magnetic specific-heat measurements. The results suggest that the short-range magnetic correlation emerges near the temperature at which magnetic susceptibility deviates from the Curie-Weiss law, and the correlation length gradually grows as the temperature is decreased. In Sec. VI, we describe the dependence of magnetic parameters including the spin-freezing temperature, T_f, and Weiss temperature, θ_W, on the glass composition and oxidation state of iron ions in the glasses. Here, it is found that the value of $|\theta_W|/T_f$ becomes lower with a decrease in $[Fe^{3+}]/[Fe_{total}]$ ratio. The decrease in $|\theta_W|/T_f$ is discussed in terms of the strong single-ion anisotropy of Fe^{2+} ions. We also discuss the effects of the single-ion anisotropy on the dynamic and static aspects of magnetic properties of the present glasses. The conclusions are summarized in Sec. VII.

II. EXPERIMENTAL PROCEDURE

Glasses with nominal compositions of $xFe_2O_3 \cdot (100\text{-}x)P_2O_5$ (x=33, 37, 40, and 45, in mol %) were prepared from reagent grade Fe_2O_3 powder and H_3PO_4 aqueous solution by using a conventional melt-quenching method. After appropriate amounts of the starting materials were mixed thoroughly, the mixture was heated at 180 °C to remove H_2O and then melted at $T_m = X$ °C (X=1200, 1350, and 1500) for 30 min in an alumina crucible. The melt was poured onto a stainless-steel plate and cooled in air. The glass samples are denoted as xFe(100-x)PX for convenience sake; for instance, 33Fe67P1200 means that the mixture with a nominal composition of $33Fe_2O_3 \cdot 67P_2O_5$ (mol %) was melted at 1200 °C. The as-quenched glass was pulverized, and then remelted in a glassy carbon crucible placed in an alumina crucible with an alumina lid at 1200 °C for 30 min in air.[13] The melt was cooled to room temperature. The glass samples melted in a glassy carbon crucible are denoted as xFe(100-x)PC (x=33, 37, and 40, in mol%). The amorphous nature of the samples was confirmed by x-ray diffraction analysis with Cu $K\alpha$ radiation. ^{57}Fe Mössbauer spectroscopy was carried out at room temperature employing ^{57}Co in metallic Rh as a γ-ray source so as to estimate valence state and coordination environment for iron ions in the glasses. The velocity scale was calibrated by using a spectrum of α-Fe measured at room temperature. Isomer shifts (IS) were given with respect to α-Fe. The temperature dependence of dc and ac susceptibilities was determined by using a Quantum Design superconducting quantum interference device magnetometer (model MPMS-XL). Specific heat was measured by a thermal relaxation method in zero magnetic field using a commercial calorimeter (Quantum Design, model PPMS).

III. ^{57}Fe MÖSSBAUER SPECTROSCOPY

The ^{57}Fe Mössbauer spectra for 33Fe67PX glasses are illustrated in Fig. 1. These spectra are explainable in terms of the superposition of paramagnetic doublets attributable to Fe^{2+} and Fe^{3+} ions. It is reasonable to presume that the absorption area ratio of paramagnetic doublets of Fe^{2+} and Fe^{3+} ions corresponds to their molar ratio. Table I summarizes the fraction of Fe^{3+} in the total number of Fe ion, $[Fe^{3+}]/[Fe_{total}]$, along with the values of Mössbauer parameters, i.e., isomer shift and quadrupole splitting (QS) for all the samples. These values were evaluated by fitting two symmetric Lorenzians to each of the paramagnetic doublets experimentally obtained. Irrespective of the value of x, $[Fe^{3+}]/[Fe_{total}]$ decreases with increasing the temperature of melting, T_m. The result is in good agreement with those reported previously.[24] A doublet of Fe^{3+} ion is not observed in the spectra of glasses melted in a glassy carbon crucible. No systematic changes are found for IS and QS when x and T_m are varied. The values of IS and QS for the Fe^{3+} and Fe^{2+} ions (IS=0.37–0.40 mm/s and QS=0.83–0.90 mm/s for Fe^{3+}; IS=1.18–1.24 mm/s and QS=2.17–2.29 mm/s for Fe^{2+}) indicate that both Fe^{3+} and Fe^{2+} ions mainly occupy octahedral sites surrounded by O^{2-} ions in the glasses, although the presence of the Fe^{3+} and Fe^{2+} ions in the tetrahedral sites cannot be ruled out.[24]

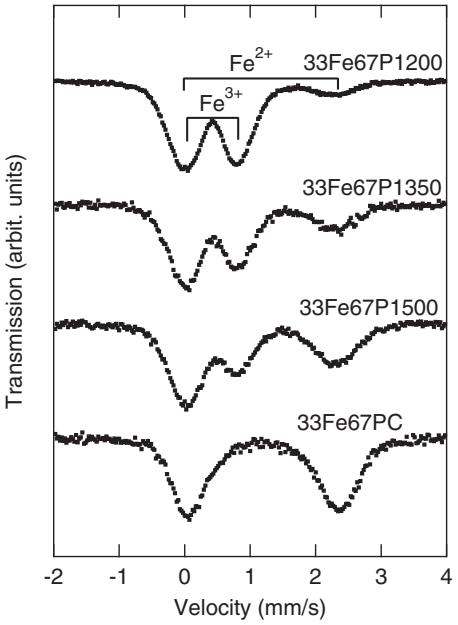

FIG. 1. ^{57}Fe Mössbauer spectra of 33Fe67PX glasses with X=1200, 1350, 1500, and C measured at room temperature. The fraction of Fe^{3+} ion in the total number of Fe ion, $[Fe^{3+}]/[Fe_{total}]$, along with the values of Mössbauer parameters, i.e., IS and QS, are summarized in Table I for all the samples.

IV. MAGNETIC PROPERTIES

A. Temperature dependence of dc magnetic susceptibility

Figures 2(a) and 2(b) show the temperature dependence of dc susceptibility $\chi(T)$ and its reciprocal $\chi^{-1}(T)$, respectively, for xFe(100-x)P1200 glasses. The inset of Fig. 2(a) depicts an enlarged view of the low-temperature region between 2 and 10 K. The measurements were performed in both field-cooling (FC) and zero-field-cooling (ZFC) processes with a

TABLE I. Parameters derived from the Mössbauer spectra and the temperature dependence of dc magnetic susceptibility for xFe(100-x)PX.

	Fe^{2+}		Fe^{3+}							
Sample	IS/mm/s	QS/mm/s	IS/mm/s	QS/mm/s	$[Fe^{3+}]/[Fe_{total}]$	T_f/K	θ_W/K	f	M_B	M_B^{theory} [a]
33Fe67P1200	1.24	2.17	0.40	0.84	0.84	4.3	−34.8	8.1	5.9	5.8
33Fe67P1350	1.20	2.24	0.40	0.84	0.63	4.5	−29.6	6.6	5.9	5.5
33Fe67P1500	1.20	2.22	0.40	0.85	0.39	4.3	−23.5	5.5	5.4	5.3
33Fe67PC	1.20	2.27			0.00	2.2	−8.6	3.9	5.6	4.8
37Fe63P1200	1.22	2.22	0.38	0.87	0.83	5.6	−45.9	8.2	5.8	5.7
37Fe63P1350	1.20	2.24	0.39	0.85	0.60	5.2	−33.4	6.4	5.7	5.5
37Fe63P1500	1.19	2.23	0.39	0.83	0.39	4.8	−25.4	5.3	5.4	5.3
37Fe63PC	1.20	2.29			0.00	2.6	−9.0	3.4	5.4	4.8
40Fe60P1200	1.21	2.17	0.37	0.89	0.83	6.2	−54.3	8.8	5.8	5.7
40Fe60P1350	1.19	2.25	0.39	0.87	0.57	6.1	−37.7	6.2	5.6	5.5
40Fe60P1500	1.20	2.22	0.38	0.88	0.38	5.5	−27.2	5.0	5.4	5.3
40Fe60PC	1.20	2.26			0.00	3.1	−11.6	3.7	5.2	4.8
45Fe55P1200	1.18	2.24	0.37	0.90	0.80	7.8	−71.9	9.2	5.8	5.7
45Fe55P1350	1.19	2.27	0.39	0.90	0.54	7.6	−51.9	6.8	5.6	5.5
45Fe55P1500	1.18	2.29	0.40	0.85	0.34	6.9	−36.0	5.2	5.4	5.2

[a] M_B^{theory} was evaluated by $M_B(Fe^{3+})\times[Fe^{3+}]/[Fe_{total}]+M_B(Fe^{2+})\times(1-[Fe^{3+}]/[Fe_{total}])$, where $M_B(Fe^{3+})$ and $M_B(Fe^{2+})$ are the ideal spin-only values of effective magnetic moment for high-spin state, i.e., 5.92 and 4.80, respectively.

magnetic field of $H=50$ Oe applied. The $\chi(T)$ curves of FC and ZFC are different from each other below the spin-freezing temperature, T_f, at which the $\chi(T)$ curve of ZFC exhibits a maximum. The spin-freezing temperature for all the glass samples is listed in Table I. The $\chi(T)$ values of FC are kept almost constant below T_f. The behavior is similar to that of typical spin glass.[25] A linear relation between $\chi^{-1}(T)$ and T at high temperatures reveals that these glasses are paramagnetic in the high-temperature region; the linear part is describable in terms of the following Curie-Weiss law

$$\frac{1}{\chi}=\frac{3k_B(T-\theta_W)}{NM_B^2\mu_B^2}, \tag{1}$$

where θ_W is the Weiss temperature, N is the number of magnetic ions per unit mass, μ_B is the Bohr magneton, M_B is the effective number of Bohr magnetons, and k_B is the Boltzmann constant. The dashed lines in Fig. 2(b) present the fitting of Eq. (1) to the experimental data of $\chi^{-1}(T)$ at temperatures from 100 to 300 K. The parameters of M_B and θ_W evaluated by the fitting are also summarized in Table I, together with the theoretical effective number of Bohr magnetons, M_B^{theory}, calculated by considering the valence states of iron ions and the spin moments for the high-spin states. The value of M_B is slightly higher than or comparable to M_B^{theory}, indicating that the orbital moments are substantially quenched by the crystal field. The negative values of θ_W indicate that the antiferromagnetic interaction is dominant among magnetic moments in the present glasses. The varia-

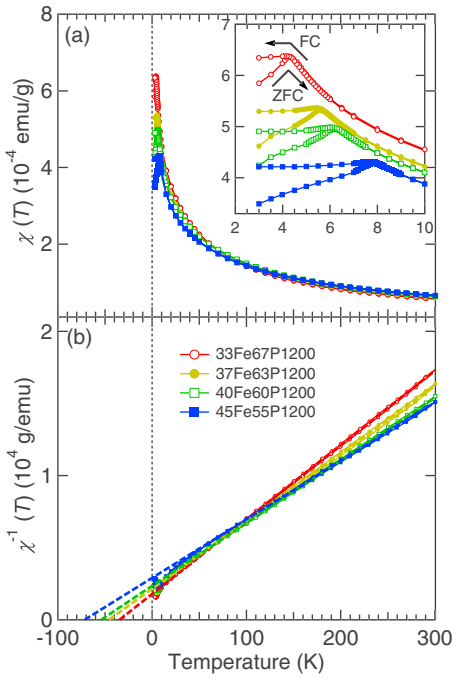

FIG. 2. (Color online) Temperature dependence of (a) dc magnetic susceptibility $\chi(T)$ and (b) its inverse $\chi^{-1}(T)$ measured at $H_{dc}=50$ Oe for the xFe(100-x)P1200 glasses with $x=33$, 37, 40, and 45. The dashed lines denote the fit of Eq. (1) to the experimental data at high temperatures.

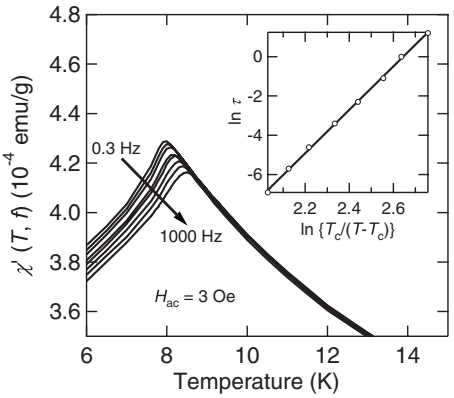

FIG. 3. Temperature dependence of real part of ac susceptibility $\chi'(T)$ at $H_{ac}=3$ Oe for 45Fe55P1200 glass. The frequency f is 0.3, 1, 3, 10, 30, 100, 300, and 1000 Hz (from top to bottom). The inset illustrates the relationship between maximum relaxation time τ and spin-freezing temperature $T_f(f)$, i.e., the analysis of critical slowing down. The solid line shows the best fit of Eq. (2) to the experimental data.

tions in T_f and θ_W with the oxidation state of iron ions, as well as those with the glass composition, are discussed in Sec. VI.

B. Dynamic scaling analysis

Figure 3 depicts the temperature dependence of real part of zero-field-cooled ac susceptibility for 45Fe55P1200 glass. The amplitude of ac magnetic field was kept at 3 Oe and the ac frequency was varied from 0.3 to 1000 Hz. As can be seen in Fig. 3, the frequency-dependent spin-freezing temperature $T_f(f)$, defined as a temperature at which the real part of ac susceptibility manifests a maximum, shifts to a higher-temperature side with an increase in f. According to the dynamic scaling hypothesis, provided that this system exhibits a conventional critical slowing down toward the transition temperature T_c, the temperature variation in relaxation time $\tau=f^{-1}$ is described by

$$\tau = \tau_0 \left(\frac{T_f(f) - T_c}{T_c} \right)^{-z\nu}, \tag{2}$$

where $z\nu$ is the dynamic exponent and τ_0 is the microscopic relaxation time. In the present case, the best fitting of Eq. (2) to the experimental data yields $z\nu=11.0$, $T_c=7.5$ K, and $\tau_0=2.1\times10^{-13}$ s, as shown in the inset of Fig. 3. The values of $z\nu=11.0$ and $\tau_0=2.1\times10^{-13}$ s are in good agreement with those reported for conventional atomic spin glasses.[26,27] For $20Fe_2O_3\cdot80TeO_2$ glass, similar values, i.e., $z\nu=10$ and $\tau_0=1.0\times10^{-13}$ s, were obtained.[9] The results of this analysis imply the occurrence of phase transition from a paramagnet to an atomic spin glass in the present iron phosphate glasses. The similar measurements and analyses have been performed for 33Fe67P1200, 33Fe67P1500, 33Fe67PC, 40Fe60PC, and 45Fe55P1500; the values of $z\nu$, T_c, and τ_0 obtained by the analysis are summarized in Table II. The values of $z\nu$ obtained for those glasses are also similar to those obtained for conventional spin glasses. One can see, however, that τ_0 varies in an enormous range over many orders of magnitude in a systematic way; with a decrease in $[Fe^{3+}]/[Fe_{total}]$, the value of τ_0 increases from $\sim10^{-13}$ to $\sim10^{-6}$ s. The value of $\tau_0=\sim10^{-6}$ s is too large and beyond the range of conventional atomic spin glasses. Not only the variation in τ_0 with $[Fe^{3+}]/[Fe_{total}]$ but also the surprisingly large value of τ_0 is discussed in terms of the effect of strong single-ion anisotropy of Fe^{2+} in Sec. VI.

TABLE II. Dynamic critical exponent $z\nu$, microscopic relaxation time τ_0, and critical temperature T_c obtained by the scaling analysis on critical slowing down using Eq. (2).

	$z\nu$	τ_0/s	T_c/K
33Fe67P1200	12.5(3)	$1.0(6)\times10^{-12}$	4.0(1)
33Fe67P1500	12.9(1)	$1.5(1)\times10^{-9}$	3.8(1)
33Fe67PC	10.4(2)	$6.2(9)\times10^{-6}$	1.9(1)
45Fe55P1200	11.0(1)	$2.1(7)\times10^{-13}$	7.5(1)
45Fe55P1500	11.4(1)	$1.3(2)\times10^{-10}$	6.5(1)
40Fe60PC	11.5(1)	$8.0(5)\times10^{-7}$	2.7(1)

C. Static scaling analysis of nonlinear susceptibility

In order to reinforce the presence of spin-glass transition in the iron phosphate glass system, the scaling analysis of static nonlinear susceptibility has been carried out for 45Fe55P1200 and 40Fe60PC glasses. We have analyzed the data concerning the temperature dependence of FC magnetization measured at various magnetic fields. Expanding $M(T,H)$ in terms of odd powers of H in a temperature regime of $T>T_f$ leads to

$$M(T,H) = \chi_0(T)H - \chi_2(T)H^3 + \chi_4(T)H^5 - \ldots, \tag{3}$$

where $\chi_0(T)$ is the linear susceptibility in the limit of $H\rightarrow0$. The static nonlinear susceptibility $\chi_{NL}(T,H)$ is defined as follows:

$$\chi_{NL}(T,H) = M(T,H)/H - \chi_0(T) = -\chi_2(T)H^2 + \chi_4(T)H^4 - \ldots. \tag{4}$$

The temperature dependence of $\chi_{NL}(T,H)$ for 45Fe55P1200 glass at varied magnetic fields is shown in the inset of Fig. 4, where $\chi_0(T)$ is taken as the dc susceptibility measured at the smallest dc magnetic field in this experiment, i.e., 20 Oe. It is found that $\chi_{NL}(T,H)$ exhibits a maximum at around T_f. A similar behavior was also seen in insulating spin glasses such as $Zn_{0.1}Mn_{0.9}In_2Te_4$.[28] It is known that the scaling analyses developed for empirical description of paramagnet-ferromagnet phase transitions provide consistent results when applied to paramagnet-spin-glass transitions. The analysis has confirmed the scaling equation,[29]

$$\chi_{NL} = -t^{\beta}\Phi\left(\frac{H^2}{t^{\beta+\gamma}}\right), \tag{5}$$

where $t=(T-T_c)/T_c$ is the reduced temperature and β and γ are the critical exponents. The universal curve resulting from the experimental data at $T>T_f$ is depicted as log-log scale

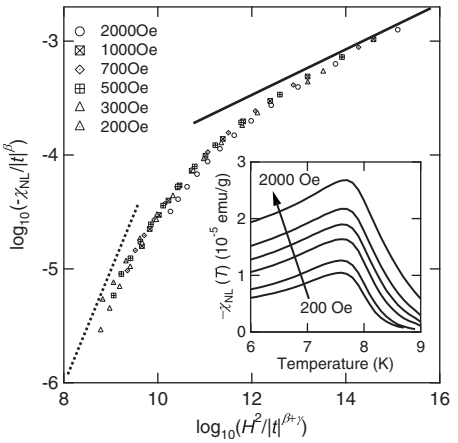

FIG. 4. Nonlinear susceptibility $\chi_{NL}(T,H)$ for 45Fe55P1200 glass analyzed according to the universal scaling function, Eq. (5). The solid and dotted lines represent the asymptotic limits; the slope of the lines is $\beta/(\beta+\gamma)$ and unity for $T\rightarrow T_f$ and $T\rightarrow\infty$, respectively. The inset shows $\chi_{NL}(T,H)$ as a function of T.

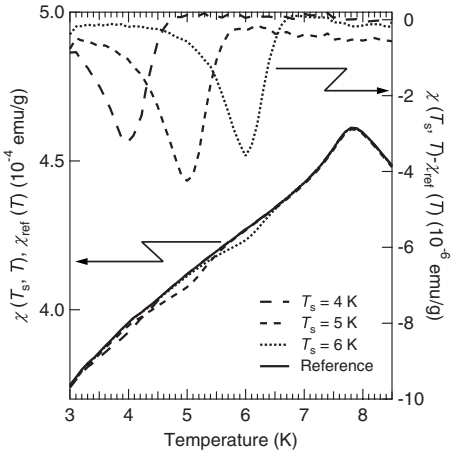

FIG. 5. Temperature dependence of dc susceptibility for 45Fe55P1200 measured on heating after ZFC with and without an intermittent stop at T_s. $\chi(T_s,T)$ and $\chi_{ref}(T)$ are the dc susceptibilities with and without the intermittent stop, respectively. The difference between $\chi(T_s,T)$ and $\chi_{ref}(T)$ is illustrated as well.

plots in Fig. 4. All the data can be suited on a single curve with T_c=7.8(1) K, β=0.9(1), and γ=3.6(2). In the case of 40Fe60PC glass, the values of T_c=2.7(1) K, β=0.9(1), and γ=3.5(3) produced the best scaling (data are not shown). The universal scaling curve covers several orders of magnitude on both ordinate and abscissa. The critical exponents obtained from the analysis are in good agreement with those reported for spin glasses with short-range interactions.[28,30–32] At temperatures sufficiently higher than T_c (lower left part of the curve), the slope approaches unity as expected. As T approaches T_c from the higher-temperature region (upper right part of the curve), the slope tends to be the proper asymptotic value $\beta/(\beta+\gamma)$.[28,30–32] The static scaling analysis of nonlinear susceptibility provides additional evidence for the presence of spin-glass transition in the iron phosphate glasses.

D. ZFC memory effects

The magnetic aging and memory effects, which are characteristic of spin glasses, have been examined for 45Fe55P1200 glass to confirm the spin-glass behavior. The ZFC memory experiment proposed by Mathieu *et al.*[2] has been performed. In this protocol, the system is cooled in zero magnetic field from a temperature higher than the transition temperature T_f with or without an intermittent stop at a stopping temperature T_s situated below T_f. The $\chi(T)$ curve is recorded during subsequent heating in a measuring magnetic field. Sasaki *et al.*[33] demonstrated theoretically and experimentally that a memory is imprinted during the aging in the absence of magnetic field only for spin glasses and strongly interacting nanoparticles systems or superspin glasses, but not for noninteracting superparamagnets. Hence, observation of the memory effect warrants the cooperative freezing of spins.

In the present case, the glass sample was cooled at a rate of 0.2 K/min from a temperature well above T_f=7.8 K to the stopping temperature T_s, which was lower than T_f, and was kept at T_s for 3 h. Here, T_s was selected to be 4, 5, and 6 K. After the aging at T_s for 3 h, the glass sample was recooled to 3 K at a rate of 0.2 K/min. Subsequently, a magnetic field of 50 Oe was applied and $\chi(T_s,T)$ was measured on heating at a rate of 0.2 K/min. As a reference, $\chi_{ref}(T)$ was determined by measuring the temperature dependence of zero-field-cooled susceptibility without any intermittent stops. Figure 5 shows the results. The $\chi(T_s,T)$ curves coincide with the $\chi_{ref}(T)$ curve in a temperature range well below T_s. The $\chi(T_s,T)$ curves deviate downward from the $\chi_{ref}(T)$ curve as the temperature becomes close to T_s. As the temperature increases in a range above T_s, the $\chi(T_s,T)$ curves rapidly approach the $\chi_{ref}(T)$ curve, and eventually merge with the $\chi_{ref}(T)$. The difference between $\chi(T_s,T)$ and $\chi_{ref}(T)$ as a function of temperature is also illustrated in Fig. 5. The effect of aging at T_s is reflected by the dip at around T_s. The experimental results definitely suggest that the magnetic phase of the present glass at very low temperatures is a spin glass.

V. MAGNETIC SPECIFIC HEAT

Magnetic specific heat, C_{mag}, has been explored for 33Fe67P1200, 33Fe67P1500, and 33Fe67PC to obtain more detailed information about the magnetic ordering in the present system. Here, we assume that the contribution of phonons to the specific heat of 33Fe67PX glasses with different molar fractions of Fe^{3+} and Fe^{2+} is identical to the sum of the specific heat of $33Ga_2O_3\cdot 67P_2O_5$ (mol %) glass multiplied by $[Fe^{3+}]/[Fe_{total}]$ and that of $33(2CaO)\cdot 67P_2O_5$ (mol %) glass multiplied by $(1-[Fe^{3+}]/[Fe_{total}])$. It is reasonable to adopt the Ga_2O_3-P_2O_5 and CaO-P_2O_5 glasses for the estimation of phonon contribution to the specific heat of Fe_2O_3-P_2O_5 and FeO-P_2O_5 glasses, respectively, because the coordination environments for Ga^{3+} and Ca^{2+} ions are similar to those for Fe^{3+} and Fe^{2+} ions, respectively, in the phosphate glasses.[34–36] The value of C_{mag} was evaluated by subtracting

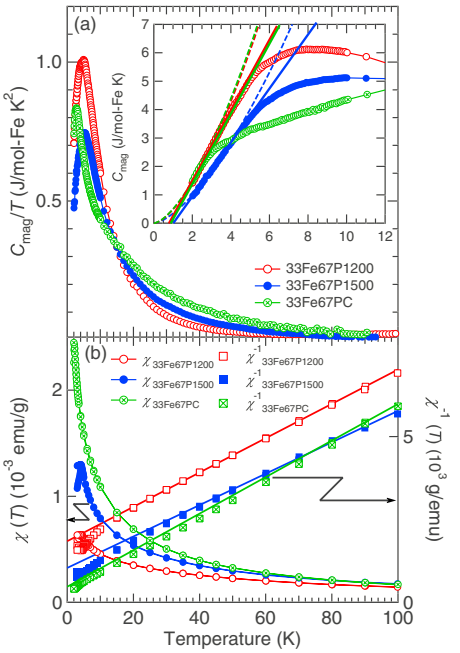

FIG. 6. (Color online) Temperature dependence of (a) magnetic specific heat divided by temperature, C_{mag}/T and (b) dc susceptibility $\chi(T)$ and its reciprocal $\chi^{-1}(T)$ for 33Fe67PX with X=1200, 1500, and C. The inset of (a) illustrates an enlarged view of C_{mag} in the low-temperature region. The solid lines and dashed curves are guides to the eyes.

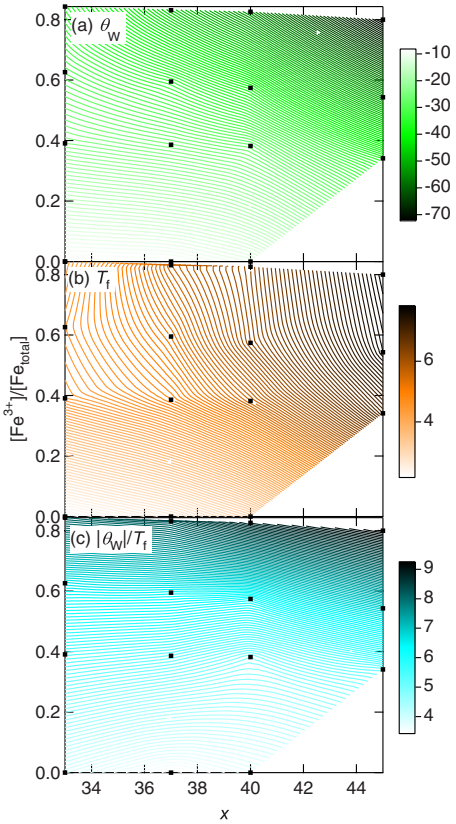

FIG. 7. (Color online) Depicted as contour plots is the dependence of Weiss temperature θ_W, spin-freezing temperature T_f, and $|\theta_W|/T_f$ on the fraction of iron ion per all cations in mol % x and the fraction of Fe^{3+} ion per total number of iron ion $[Fe^{3+}]/[Fe_{total}]$. Closed squares indicate the experimental data, based on which the contour plots are illustrated.

the contribution of phonons from the total specific heat. In the inset of Fig. 6(a), C_{mag} per 1 mol of iron ion is plotted as a function of T in a temperature regime of 2 to 12 K. The temperature dependence of C_{mag} for 33Fe67P1200, 33Fe67P1500, and 33Fe67PC shows very diffused peaks at 8, 10, and 22 K, corresponding to $1.9T_f$, $2.3T_f$, and $10T_f$, respectively. The broad maxima of C_{mag} at temperatures much higher than T_f are characteristic of spin glasses.[8,37,38] At low temperatures well below the peak temperature, C_{mag} is proportional to temperature with a positive intercept on the temperature axis [see the solid lines of the inset of Fig. 6(a)]. This behavior was also observed in conventional spin glasses.[37,38] An alternative view is that C_{mag} is proportional to T^α with α=1.5–1.6 for the present glasses at low temperatures [see the dashed curves of Fig. 6(a)] In general, $C_{mag} \propto T^{1.5}$ is expected from the spin-wave theory of ferromagnets. However, the $T^{1.5}$ dependence of C_{mag} was reported for some magnets that exhibit spin-glass behavior such as $Yb_2Mn_2O_7$ and $Na_{0.70}MnO_2$.[39–41] The quantity, C_{mag}/T, is plotted as a function of T in Fig. 6(a). Figure 6(b) illustrates the temperature dependence of $\chi(T)$ and $\chi^{-1}(T)$ for the present glasses. The temperature dependence of C_{mag}/T exhibits a peak at around T_f ($1.1T_f$–$1.2T_f$). In a high-temperature regime, C_{mag}/T is equal to zero and $\chi^{-1}(T)$ shows the Curie-Weiss behavior. With lowering the temperature, $\chi(T)$ begins to deviate from the Curie-Weiss law, accompanied by the onset of C_{mag}/T. This indicates that the short-range magnetic correlation emerges at temperatures higher by one order of magnitude than T_f, which is a clear signature of the magnetic frustration. At around 90 K, the magnetic entropy calculated by integrating C_{mag}/T for T reaches values between R ln 6 and R ln 5 expected from the degree of freedom for spins of Fe^{3+} and Fe^{2+}, respectively, where R is the gas constant.

VI. EFFECTS OF SINGLE-ION ANISOTROPY ON MAGNETIC PROPERTIES

As demonstrated above, the iron phosphate glasses exhibit transitions into spin-glass phases at low temperatures. We consider the effects of composition and valence state of iron ions on the magnetic properties. First, we discuss the magnetic parameters such as the spin-freezing temperature and Weiss temperature obtained by the temperature dependence of dc magnetic susceptibility (See Sec. IV A). Figures 7(a) and 7(b) illustrate contour plots of θ_W and T_f, respectively, on the x-$[Fe^{3+}]/[Fe_{total}]$ planes. According to the high-temperature approximation of mean-field theory, θ_W, a parameter reflecting the magnitude of the molecular field, is proportional to $J_{eff}NM_B^2$, where J_{eff} is the effective exchange integral. In the present case, x is directly related to N. The value of $[Fe^{3+}]/[Fe_{total}]$ is relevant to M_B; the Fe^{2+} and Fe^{3+} ions have the electron configurations of $3d^6$ and $3d^5$, leading to S=2 and S=5/2 in their high-spin states, respectively. So, the mean value of M_B increases with increasing

$[Fe^{3+}]/[Fe_{total}]$. The value of $[Fe^{3+}]/[Fe_{total}]$ also affects the magnitude of J_{eff}. The effective exchange integral of superexchange interaction via an oxide ion derived from the third-order perturbation is proportional to $J_{pd}|t|^2/(\Delta E)^2$, where J_{pd} is the coupling constant of direct exchange interaction between the magnetic cations and the oxide ions, t is the transfer integral related to hopping of the electron between the $3d$ orbitals of magnetic cations and the $2p$ orbitals of oxide ion, and ΔE is the excitation energy. These three parameters, J_{pd}, t, and ΔE, depend on the valence state of iron ions. Taking into account the fact that Fe^{3+}-based magnetic crystalline oxides usually have stronger superexchange interactions than Fe^{2+}-based ones, it is anticipated that in the present glasses the averaged value of $|J_{eff}|$ becomes larger with an increase in $[Fe^{3+}]/[Fe_{total}]$. The above discussion leads to the conclusion that the value of $|\theta_W|$ becomes larger with increasing x and $[Fe^{3+}]/[Fe_{total}]$. The similar tendency is anticipated for T_f, although it is too difficult to formulate the spin-freezing temperature of spin glasses. As seen in Fig. 7(a), $|\theta_W|$ exhibit an increase when x or $[Fe^{3+}]/[Fe_{total}]$ is higher; the higher values of $|\theta_W|$ are found in upper right part of Fig. 7(a). On the other hand, the variation in T_f on the x-$[Fe^{3+}]/[Fe_{total}]$ plane is rather different from that of $|\theta_W|$; T_f tends to be higher with an increase in x while it just slightly depends on $[Fe^{3+}]/[Fe_{total}]$, as shown in Fig. 7(b). This is not in agreement with the above rough estimation.

Here we introduce the parameter, $|\theta_W|/T_f$, in order to clarify another factor that affects the spin-freezing temperature. The contour plot of $|\theta_W|/T_f$ on the x-$[Fe^{3+}]/[Fe_{total}]$ plane is shown in Fig. 7(c). It should be noted that $|\theta_W|/T_f$ approximately depends only on $[Fe^{3+}]/[Fe_{total}]$ and becomes smaller when $[Fe^{3+}]/[Fe_{total}]$ is decreased, indicating that the occurrence of magnetic transition tends to be favored when $[Fe^{3+}]/[Fe_{total}]$ becomes lower. This tendency is considered to be relevant to the difference in single-ion anisotropy between Fe^{2+} and Fe^{3+} ions. Introducing spin-orbital coupling as second-order perturbation, magnetic ions such as Fe^{2+} and Co^{2+} have significant single-ion anisotropy even if they have nondegenerate ground states of electronic configuration due to the crystal-field effects.[42,43] Assuming that the exchange interaction is isotropic, i.e., Heisenberg-type, the single-ion anisotropy is introduced into the Hamiltonian as follows:

$$H = -\sum_{(i,j)} J_{ij} S_i \cdot S_j + \sum_i D_i (S_i^Z)^2, \tag{6}$$

where J_{ij} is the exchange coupling constant between the sites i and j, S_i is the spin operator at the site i, D_i is the single-ion anisotropy constant at the site i, and S_i^Z is the component of spin operator along the direction of the easy axis or perpendicular to the easy plane at the site i. The single-ion anisotropy term suppresses the fluctuation of magnetic moments caused by the thermal energy, so that the spin-freezing temperature is apt to be increased by the presence of the anisotropy. The effects of single-ion anisotropy are expected to be stronger for Fe^{2+} ion than for Fe^{3+} ion, although the existence of finite single-ion anisotropy effects is revealed even for S-state ions such as Fe^{3+} and Gd^{3+}.[44,45] Thus, from the point of view of fluctuation, the value of $|\theta_W|/T_f$ decreases when $[Fe^{3+}]/[Fe_{total}]$ is lower.

On the other hand, the ratio of the absolute value of Weiss temperature to Néel temperature is regarded as an empirical measure of magnetic frustration for a number of geometrically frustrated antiferromagnets.[46] In the present glasses, the value of $|\theta_W|/T_f$ is sufficiently larger than unity, implying that the present system is magnetically frustrated. However, we must consider the effect of single-ion anisotropy on the magnetic frustration. It is thought that the single-ion anisotropy enhances the magnetic frustration since it becomes more difficult for the system to minimize the local exchange energies when the orientations of the magnetic moments are restricted. Besides, since the spatial distribution of Fe^{3+} and Fe^{2+} ions affects the strength of exchange interactions, the change in $[Fe^{3+}]/[Fe_{total}]$ can alter the degree of magnetic frustration in an intricate and, possibly, nonmonotonous way. Considering the fact that $|\theta_W|/T_f$ decreases with a decrease in $[Fe^{3+}]/[Fe_{total}]$ [see Fig. 7(c)], it is speculated that the single-ion anisotropy of Fe^{2+} has more significant influence on the fluctuation of magnetic moments rather than the magnetic frustration.

The suppression of spin fluctuation due to the single-ion anisotropy influences the spin dynamics, as discussed for molecular magnets.[47,48] If we assume the uniaxial single-ion anisotropy for Fe^{2+} ion, the temperature dependence of microscopic relaxation time of Fe^{2+} ion is expected to be expressed as follows:[47,48]

$$\tau_{0i}(T) = \tau_0^* \exp\left(\frac{|D_i|S_i^2}{k_B T}\right), \tag{7}$$

where τ_0^* is the relaxation time for spin flipping in the absence of energy barrier. Namely, the single-ion anisotropy is introduced as a thermal activation energy. For instance, crystalline lithium iron phosphate ($LiFePO_4$) has a single-ion anisotropy with an easy axis.[42,43] The single-ion anisotropy leads to the slowing down in the flipping of magnetic moments. In the present case, the value of τ_0 increases from $\sim 10^{-13}$ to $\sim 10^{-6}$ s with a decrease in $[Fe^{3+}]/[Fe_{total}]$ (see Table II). However, it is difficult to analyze the temperature dependence of τ of 33Fe67PC and 40Fe60PC quantitatively using the equation derived by combining Eqs. (2) and (7), partly because D_i has a wide distribution depending on the Fe^{2+} site due to the random structure of glasses so that the temperature dependence of averaged value of τ_0 shows complicated behavior. Thus, the dependences of $|\theta_W|/T_f$ and τ_0 on $[Fe^{3+}]/[Fe_{total}]$ are just qualitatively explained by the single-ion anisotropy of Fe^{2+} ion.

The critical exponents of $\beta=0.9(1)$ and $\gamma=3.5(3)$ obtained in the static scaling analysis of nonlinear susceptibility for 40Fe60PC glass (see Sec. IV C) are similar to those reported for many three-dimensional (3D) Heisenberg spin-glass systems with short-range interactions, rather than 3D Ising spin glass such as $Fe_{0.5}Mn_{0.5}TiO_3$, for which $\beta=0.54$ and $\gamma=4.0$.[49] In the present system, each magnetic moment of Fe^{2+} should exhibit the Ising-like behavior due to the strong single-ion anisotropy, but the orientation of easy axis of single-ion anisotropy has a wide distribution due to the random structure of glasses. Hence, it does not seem that the present glasses, even when they contain only Fe^{2+} ions, are

regarded as the simple Ising spin system. The Fe^{2+}-based glasses are interesting as a model for 3D spin-glass system with antiferromagnetic interactions and random anisotropy.

VII. CONCLUSIONS

The magnetic properties of mixed-valence iron phosphate glasses have been investigated. The scaling analyses of relaxation time and nonlinear susceptibility yield critical exponents similar to those reported for conventional spin glasses, indicating the presence of spin-glass transition at low temperatures. The observation of magnetic aging and memory effects reinforces the spin-glass nature of the present glasses. The experimental data of magnetic specific heat reveal that the deviation of magnetic susceptibility from the Curie-Weiss law corresponds to the emergence of short-range magnetic correlation. The single-ion anisotropy of iron ions plays an important role in both static and dynamic aspects of magnetic properties. In particular, the single-ion anisotropy leads to the suppression of spin fluctuation, resulting in the decrease in $|\theta_W|/T_f$ and increase in τ_0 with a decrease in $[Fe^{3+}]/[Fe_{total}]$.

ACKNOWLEDGMENTS

The authors would like to thank M. Tosaki of Radioisotope Research Center, Kyoto University for the Mössbauer-effect measurements. The authors also thank M. Azuma and Y. Shimakawa of the Institute of Chemical Research, Kyoto University for specific-heat measurements. This research was partially supported by the Ministry of Education, Science, Sports and Culture, Grant-in-Aid for Scientific Research (B) (Grant No. 19360298) and Challenging Exploratory Research (Grant No. 21656163). One of authors (H.A.) thanks the Grant-in-Aid for Fellow (Grant No. 20-6726) from Japan Society for the Promotion of Science (JSPS).

*Corresponding author; tanaka@dipole7.kuic.kyoto-u.ac.jp

[1] V. Cannella and J. A. Mydosh, Phys. Rev. B **6**, 4220 (1972).
[2] R. Mathieu, P. Jönsson, D. N. H. Nam, and P. Nordblad, Phys. Rev. B **63**, 092401 (2001).
[3] K. Jonason, E. Vincent, J. Hammann, J. P. Bouchaud, and P. Nordblad, Phys. Rev. Lett. **81**, 3243 (1998).
[4] L. W. Bernardi, H. Yoshino, K. Hukushima, H. Takayama, A. Tobo, and A. Ito, Phys. Rev. Lett. **86**, 720 (2001).
[5] S. Miyashita and E. Vincent, Eur. Phys. J. B **22**, 203 (2001).
[6] P. E. Jönsson, R. Mathieu, P. Nordblad, H. Yoshino, H. A. Katori, and A. Ito, Phys. Rev. B **70**, 174402 (2004).
[7] J. J. Hopfield, Proc. Natl. Acad. Sci. U.S.A. **79**, 2554 (1982).
[8] J. A. Mydosh, *Spin Glasses: An Experimental Introduction* (Taylor & Francis, London, 1993).
[9] H. Akamatsu, K. Tanaka, K. Fujita, and S. Murai, Phys. Rev. B **74**, 012411 (2006).
[10] C. Dupas, J. P. Renard, G. Fonteneau, and J. Lucas, J. Magn. Magn. Mater. **27**, 152 (1982).
[11] F. A. Wedgwood and A. C. Wright, J. Non-Cryst. Solids **21**, 95 (1976).
[12] J. L. Shaw, A. C. Wright, R. N. Sinclair, G. K. Marasinghe, D. Holland, M. R. Lees, and C. R. Scales, J. Non-Cryst. Solids **345-346**, 245 (2004).
[13] H. Akamatsu, K. Fujita, S. Murai, and K. Tanaka, Appl. Phys. Lett. **92**, 251908 (2008).
[14] R. A. Verhelst, R. W. Kline, A. M. de Graaf, and H. O. Hooper, Phys. Rev. B **11**, 4427 (1975).
[15] J. Ferre, J. Pommier, J. P. Renard, and K. Knorr, J. Phys. C **13**, 3697 (1980).
[16] A. Ito, E. Torikai, H. Yamauchi, and Y. Shono, J. Phys. C **15**, 2759 (1982).
[17] J. P. Sanchez and J. M. Friedt, J. Phys. (Paris) **43**, 1707 (1982).
[18] J. P. Sanchez, J. M. Friedt, R. Horne, and A. J. Van Duyneveldt, J. Phys. C **17**, 127 (1984).
[19] P. Beauvillain, C. Dupas, J. P. Renard, and P. Veillet, Phys. Rev. B **29**, 4086 (1984).
[20] K. Tanaka, H. Akamatsu, S. Nakashima, and K. Fujita, J. Non-Cryst. Solids **354**, 1347 (2008).
[21] H. Akamatsu, K. Tanaka, K. Fujita, and S. Murai, J. Phys.: Condens. Matter **20**, 235216 (2008).
[22] H. Akamatsu, S. Murai, K. Fujita, and K. Tanaka, Adv. Mater. Res. **39-40**, 207 (2008).
[23] H. Akamatsu, K. Tanaka, K. Fujita, and S. Murai, J. Magn. Magn. Mater. **310**, 1506 (2007).
[24] M. Karabulut, G. K. Marasinghe, C. S. Ray, D. E. Day, G. D. Waddill, C. H. Booth, P. G. Allen, J. J. Bucher, D. L. Caulder, and D. K. Shuh, J. Non-Cryst. Solids **306**, 182 (2002).
[25] S. Nagata, P. H. Keesom, and H. R. Harrison, Phys. Rev. B **19**, 1633 (1979).
[26] K. Gunnarsson, P. Svedlindh, P. Nordblad, L. Lundgren, H. Aruga, and A. Ito, Phys. Rev. Lett. **61**, 754 (1988).
[27] P. Nordblad, J. Phys.: Condens. Matter **16**, S715 (2004).
[28] G. F. Goya and V. Sagredo, Phys. Rev. B **64**, 235208 (2001).
[29] M. Suzuki, Prog. Theor. Phys. **58**, 1151 (1977).
[30] P. M. Shand, A. D. Christianson, T. M. Pekarek, L. S. Martinson, J. W. Schweitzer, I. Miotkowski, and B. C. Crooker, Phys. Rev. B **58**, 12876 (1998).
[31] P. Beauvillain, C. Chappert, J. P. Renard, and J. Seiden, J. Magn. Magn. Mater. **54-57**, 127 (1986).
[32] A. Mauger, J. Ferre, and P. Beauvillain, Phys. Rev. B **40**, 862 (1989).
[33] M. Sasaki, P. E. Jönsson, H. Takayama, and H. Mamiya, Phys. Rev. B **71**, 104405 (2005).
[34] E. Matsubara, Y. Waseda, M. Ashizuka, and E. Ishida, J. Non-Cryst. Solids **103**, 117 (1988).
[35] D. Ilieva, B. Jivov, C. Petkov, I. Penkov, and Y. Dimitriev, J. Non-Cryst. Solids **283**, 195 (2001).
[36] D. M. Pickup, R. M. Moss, D. Qiu, R. J. Newport, S. P. Valappil, J. C. Knowles, and M. E. Smith, J. Chem. Phys. **130**, 064708 (2009).
[37] L. E. Wenger and P. H. Keesom, Phys. Rev. B **13**, 4053 (1976).
[38] G. W. Hunter, L. E. Wenger, and W. D. Wallace, Phys. Rev. B **36**, 5750 (1987).
[39] J. E. Greedan, N. P. Raju, A. Maignan, Ch. Simon, J. S. Peder-

sen, A. M. Niraimathi, E. Gmelin, and M. A. Subramanian, Phys. Rev. B **54**, 7189 (1996).
[40] L. B. Luo, Y. G. Zhao, G. M. Zhang, S. M. Guo, Z. Li, and J. L. Luo, Phys. Rev. B **75**, 125115 (2007).
[41] N. A. Chernova, J. K. Ngala, P. Y. Zavalij, and M. S. Whittingham, Phys. Rev. B **75**, 014402 (2007).
[42] J. Li, V. O. Garlea, J. L. Zarestky, and D. Vaknin, Phys. Rev. B **73**, 024410 (2006).
[43] G. Liang, K. Park, J. Li, R. E. Benson, D. Vaknin, J. T. Markert, and M. C. Croft, Phys. Rev. B **77**, 064414 (2008).
[44] R. S. Fishman, J. Appl. Phys. **103**, 07B109 (2008).
[45] J. A. Quilliam, K. A. Ross, A. G. Del Maestro, M. J. P. Gingras, L. R. Corruccini, and J. B. Kycia, Phys. Rev. Lett. **99**, 097201 (2007).
[46] A. P. Ramirez, Annu. Rev. Mater. Sci. **24**, 453 (1994).
[47] C. Coulon, R. Clérac, L. Lecren, W. Wernsdorfer, and H. Miyasaka, Phys. Rev. B **69**, 132408 (2004).
[48] M. Mito, H. Deguchi, T. Tajiri, S. Takagi, M. Yamashita, and H. Miyasaka, Phys. Rev. B **72**, 144421 (2005).
[49] K. Gunnarsson, P. Svedlindh, P. Nordblad, L. Lundgren, H. Aruga, and A. Ito, Phys. Rev. B **43**, 8199 (1991).